



**A method to
enhance near
saturation functions?**

E. Beckers et al.

Coupling X-ray microtomography and macroscopic soil measurements: a method to enhance near saturation functions?

E. Beckers¹, E. Plougonven^{2,*}, N. Gigot¹, A. Léonard², C. Roisin³, Y. Brostaux⁴, and A. Degré¹

¹Univ. Liège, GxABT, Soil – Water Systems, 2 Passage des Déportés, 5030 Gembloux, Belgium

²Univ. Liège, Department of Applied Chemistry, Laboratory of Chemical Engineering, Sart-Tilman, 4000 Liège, Belgium

³Walloon Agricultural Research Centre of Gembloux (CRA-W), Department of Agriculture and Natural Environment, Soil Fertility and Water Protection Unit, 4 Rue du Bordia, 5030 Gembloux, Belgium

⁴Univ. Liège, GxABT, Applied Statistics, Computer Science and Mathematics Unit, 2 Passage des Déportés, 5030 Gembloux, Belgium

*now at: ICMCB-CNRS/Group 4, 87 Avenue du Docteur Albert Schweitzer, 33608 Pessac, France

Title Page

Abstract

Introduction

Conclusions

References

Tables

Figures

⏪

⏩

◀

▶

Back

Close

Full Screen / Esc

Printer-friendly Version

Interactive Discussion



Received: 27 February 2013 – Accepted: 2 April 2013 – Published: 15 April 2013

Correspondence to: E. Beckers (eleonore.beckers@ulg.ac.be)

Published by Copernicus Publications on behalf of the European Geosciences Union.

HESSD

10, 4799–4827, 2013

A method to enhance near saturation functions?

E. Beckers et al.

Title Page

Abstract

Introduction

Conclusions

References

Tables

Figures



Back

Close

Full Screen / Esc

Printer-friendly Version

Interactive Discussion



Abstract

Agricultural management practices influence soil structure, but the characterization of these modifications and consequences are still not completely understood. In this study, we aim at improving water retention and hydraulic conductivity curves using both classical soil techniques and X-ray microtomography in the context of tillage simplification. We show a good match for retention and conductivity functions between macroscopic measurements and microtomographic information. Microtomography highlights the presence of a secondary pore system. Analysis of structural parameters for these pores appears to be significant and offers additional clues for objects differentiation. We show that relatively fast scans supply not only good results, but also enhance near saturation characterization, making microtomography a highly competitive instrument for routine soil characterization.

1 Introduction

Tillage simplification becomes a popular practice in recent years. Different reasons are at the origin of this phenomenon, notably energy saving, decreasing soil erosion, etc. Agricultural management practices influence soil structure – a great number of papers in the literature shows the effects of tillage intensity on soil (see Strudley et al., 2008, for a review on the subject) – but changes in soil hydrodynamic behaviour at the field scale are still not fully understood. Moreover, research shows divergent conclusions over the impact on soil hydraulic properties; some papers and reviews have already reported these divergences (e.g. Green et al., 2003; Cousin et al., 2004; Batthacharyya et al., 2006; Strudley et al., 2008). However, for the most part, studies agree with the fact that soil structure and more precisely pore size distribution, connectivity and orientation are impacted. These changes in porosity-related properties lead to a quantitative modification of the water fluxes and their partition. But the characterization of these modifications and consequences remains a challenge.

HESSD

10, 4799–4827, 2013

**A method to
enhance near
saturation functions?**

E. Beckers et al.

Title Page

Abstract

Introduction

Conclusions

References

Tables

Figures

◀

▶

◀

▶

Back

Close

Full Screen / Esc

Printer-friendly Version

Interactive Discussion



HESSD

10, 4799–4827, 2013

A method to enhance near saturation functions?

E. Beckers et al.

[Title Page](#)

[Abstract](#)

[Introduction](#)

[Conclusions](#)

[References](#)

[Tables](#)

[Figures](#)

[⏪](#)

[⏩](#)

[◀](#)

[▶](#)

[Back](#)

[Close](#)

[Full Screen / Esc](#)

[Printer-friendly Version](#)

[Interactive Discussion](#)



Many studies focus only on one kind of measurement: in-situ for the macroscopic scale, or in the laboratory at the soil sample scale. Plot scale measurements allow characterization of the global behaviour, but do not provide mechanistic explanations of the hydrodynamic modifications. In fact, the divergence in the literature in regards to agricultural management impacts shows the inability of these measurements to comprehend them completely. On the contrary, microscale characterization, involving small soil samples and accuracy to within a micron or less, can offer helpful insight on the pore structure, but might not be representative at the plot scale. Notably, X-ray tomography has been recently used in order to characterize changes in soil pore distribution in different contexts. In 1997 already, Olsen and Borresen (1997) were studying pore characteristics depending on tillage intensity with computed tomography. However, at that time, the pixel size was about 0.5 mm. With this resolution, they could only conclude about the macroporosity distribution in the soil profile. Since Olsen and Borresen (1997), soil porosity was analyzed many times thanks to X-ray tomography (see Taina et al., 2008 for a state of the art), but research on the link between macroscopic measurements and microscopic investigation of the soil structure remain scarce. In 2000, Wiermann et al. (2000) showed the interest of this technique by combining water retention, hydraulic conductivity and tomography analyses to compare soil reaction to pre-compression stress depending on management practices. Kumar et al. (2010) and Kim et al. (2010) tried to explain saturated hydraulic conductivity (K_{sat}) differences by pore parameter measurements with computed tomography, and found that most of these parameters were correlated with K_{sat} . Rachman et al. (2005) and Quinton et al. (2009) studied macroporosity through X-ray tomography and water retention curves; they concluded that these methods lead to comparable results for porosity distributions. Dal Ferro et al. (2012), for their part, analyzed soil porosity with mercury intrusion porosimetry and X-ray microtomography. They highlighted the fact that microtomography does not take into account all the microporosity, and therefore advised to combine microtomography analyses with other techniques. Cousin et al. (2004) conducted a two-scale study in order to determine more parameters: qualitative observation of macroporosity

HESSD

10, 4799–4827, 2013

A method to enhance near saturation functions?

E. Beckers et al.

[Title Page](#)[Abstract](#)[Introduction](#)[Conclusions](#)[References](#)[Tables](#)[Figures](#)[⏪](#)[⏩](#)[◀](#)[▶](#)[Back](#)[Close](#)[Full Screen / Esc](#)[Printer-friendly Version](#)[Interactive Discussion](#)

through stained infiltration combined with laboratory hydraulic conductivity measurements and tomographic analyses. They reported a better plot conductivity in no tillage due to the presence of earthworm tunnels. The scarcity of these tunnels leads to the need for macroscopic measurements while tomographic observations allow a quantitative characterization of the bulk soil pore network. However, the achieved resolution in their study (i.e. 0.4 mm pixel size) wasn't sufficient to confirm a link between the pore network and in-situ hydraulic conductivity measurements. Finally, Bayer et al. (2004) tested the ability of microtomography to provide water retention curves through a dynamic setup. Their results were in good agreement with a classical multistep outflow experiment. We can see that microtomography becomes an interesting tool in the study of soil pore networks, as it provides a 3-D visualization of the internal soil structure and can allow us to refine our knowledge on hydraulic and retention functions at near saturation. Further than pore size distribution, microtomography offers the possibility to extract a multitude of other structural parameters. Among them, pore connectivity, which influences hydrodynamics (Vogel and Roth, 1998), or specific surface (surface area/volume) (Gerke, 2012) can be estimated. However, the consistency of the results depends on the quality of the tomographic reconstructions. Quality is, among other factors, correlated with acquisition time, and as a result microtomography as a hydraulic measurement technique is considered as time-consuming in comparison with other measuring techniques.

In our study, we show that relatively fast scans supply not only good results, but also enhance near saturation characterization. These elements make microtomography a highly competitive instrument for routine soil characterization. In this paper, we aim at testing X-ray microtomography as a tool to help differentiate – if not quantify – soil structure modification depending on tillage intensity through coupled macro- and microscopic measurements. This association could help highlight the most influential microstructural factors affecting macroscopic transport phenomena. Water retention and hydraulic conductivity curves, 3-D soil strength profiles and X-ray microtomography (34 μm pixel size) compose the experimentation campaign. Concurring mastered

and redundant macroscopic observations enable to control microtomographic results and to use the latter as an explanatory element of the fundamental processes highlighted by macroscopic measurements.

2 Material and methods

5 Macroscopic investigations include 3-D soil strength profiles, retention data with Richards' apparatus, saturated and unsaturated soil conductivity. Microscopic investigations consist in measuring 3-D morphological parameters using X-ray microtomography (μ CT).

10 Retention and hydraulic curves are derived from and compared for both macroscopic and microscopic investigations. Morphological parameters are analyzed with principal component analysis.

2.1 Location

Our field experiment takes place in Gentinnes (Wallon Brabant, Belgium), on a field organized in a Latin square scheme. Since 2004, plots have been cultivated in conventional tillage (CT), deep loosening (not studied here), or in reduced tillage (RT).
15 The latter consists in sowing after stubble ploughing of about 10 cm. Because of the variation in tillage depth between management practices (10 cm for RT vs. 25 cm for CT), two horizons are investigated for RT: RT1 between 0–10 cm and RT2 between 12–25 cm (see Fig. 1). The crop rotation is sugar beet – winter wheat – flax. The soil is
20 mainly composed of silt loam and can be classified as a Luvisol.

HESSD

10, 4799–4827, 2013

A method to enhance near saturation functions?

E. Beckers et al.

Title Page

Abstract

Introduction

Conclusions

References

Tables

Figures

◀

▶

◀

▶

Back

Close

Full Screen / Esc

Printer-friendly Version

Interactive Discussion



2.2 Measurements techniques

2.2.1 Penetrometry

A fully automated penetrometer (30° angle cone with a base area of 10 mm²) mounted on a small vehicle is used. With this equipment, we cover a 160 × 80 cm² area, which we estimate to be sufficiently wide to evaluate the effect of the most commonly used tillage implements. At each node (with 5 cm spacing between neighbouring points), a penetration is performed, and data are collected every 1 cm from 5 cm to 55 cm depth. More information can be found in Roisin (2007).

2.2.2 Water retention

Retention points (between pF 1 to 4.2) are obtained thanks to the Richards' procedure on one hand (1948; Dane and Hopmans, 2002 cited by Solone et al., 2012): samples are saturated by upward moisturizing for 48 h, and then exposed to increasing pressures and weighed between each stage. Seven soil samples (100 cm³) are removed from each horizon (CT, RT1 and RT2).

Pore size distribution is, on the other hand, derived from tomographic results (see Sect. 2.2.4) and allows to calculate retention data points (between pF 1 and saturation) using the following relationship (capillary theory, Jurin's law) between radius, r (L) and pressure head, h (L):

$$r = \frac{2\sigma\cos(\alpha)}{\rho gh} \quad (1)$$

Where σ is the liquid surface tension (M T⁻²), α is the contact angle between the liquid and the soil, ρ is the liquid density (M L⁻³) and g is the gravitational acceleration (L T⁻²).

HESSD

10, 4799–4827, 2013

A method to enhance near saturation functions?

E. Beckers et al.

Title Page

Abstract

Introduction

Conclusions

References

Tables

Figures

◀

▶

◀

▶

Back

Close

Full Screen / Esc

Printer-friendly Version

Interactive Discussion



2.2.3 Hydraulic conductivity

In situ measurements

In situ infiltration measurements are performed by a 20 cm diameter tension-infiltrometer (TI) (Eijkelkamp Agrisearch Equipment). Eight repetitions are made for each management practice. For each location, three to four infiltration measurements for tensions between -10 and -3 cm are performed. Measurements are long enough to have at least 18 min of steady-state infiltration. We only use the unsaturated flows, saturated hydraulic conductivity being measured directly in the laboratory.

Laboratory measurements

We use a permeameter (Laboratory-Permeameter, Eijkelkamp, Giesbeek, Netherlands) to measure saturated hydraulic conductivity on 100 cm^3 soil samples. The basic principle is to create a pressure gradient between the sides of the sample and to measure the flow coming out. The constant head method is used (Klute, 1986 cited by Bayer et al., 2004). Considering the possible change in pore orientation, we measure this conductivity in the two main orientations: vertical conductivity vs. horizontal conductivity (parallel to the slope). Measurements are performed on 8 samples for each object (CT, RT1 and RT2) and each orientation. In this paper, we only use the highest value for each management practice and associate this value to the macroporosity determined by other measurements.

Hydraulic macroporosity efficiency

Following Watson and Luxmoore (1986, cited by Imhoff et al., 2010), the number of hydraulically effective pores between two tensions is related to the difference between hydraulic conductivity for these two tensions (K_m , L T^{-1}) and can be calculated thanks to Poiseuille's law and laminar flow equation:

A method to enhance near saturation functions?

E. Beckers et al.

Title Page

Abstract

Introduction

Conclusions

References

Tables

Figures

⏪

⏩

◀

▶

Back

Close

Full Screen / Esc

Printer-friendly Version

Interactive Discussion



$$N_m = \frac{8\eta K_m}{\pi \rho g r_a^4} \quad (2)$$

Where η is the water dynamic viscosity ($\text{ML}^{-1} \text{T}^{-1}$) and r_a is the minimum pore radius (L). The associated macroporosity is equivalent to:

$$\theta_m = N_m \pi r_a^2 \quad (3)$$

- 5 The ratio between effective macroporosity and measured porosity is therefore an indicator of the hydraulic performances of the soil (Buczko et al., 2006, cited by Imhoff et al., 2010), and will be tested in our context.

2.2.4 X-ray microtomography

10 X-ray microtomography consists in performing a series of X-ray radiograms under different angles, producing enough information to algorithmically reconstruct a 3-D X-ray attenuation map of the sample. The transmitted X-ray intensity depends on the attenuation coefficient of each material located along the X-ray path, in a cumulative way. The attenuation coefficient is related to the material properties, i.e. its density and atomic number (Attix and Roesch, 1968) and to the energy of the incident beam.

15 Sampling

Soil sample dimensions have been chosen according to the tomograph characteristics. The cylindrical samples are 5 cm in height and 3 cm in diameter, allowing for a good compromise between resolution and time acquisition.

X-ray microtomograph

20 Samples are scanned using a Skyscan-1172 high-resolution desktop micro-CT system (Skyscan, Kontich, Belgium). The cone beam source operates at 100 kV, and an aluminium filter is used. The detector configuration (16-bit X-ray camera with 2×2 binning,

A method to enhance near saturation functions?

E. Beckers et al.

Title Page

Abstract

Introduction

Conclusions

References

Tables

Figures

◀

▶

◀

▶

Back

Close

Full Screen / Esc

Printer-friendly Version

Interactive Discussion



HESSD

10, 4799–4827, 2013

A method to enhance near saturation functions?

E. Beckers et al.

Title Page

Abstract

Introduction

Conclusions

References

Tables

Figures

◀

▶

◀

▶

Back

Close

Full Screen / Esc

Printer-friendly Version

Interactive Discussion



creating 2048 × 1024 pixel radiograms) and the distance source-object-camera are adjusted to produce images with a pixel size of 34 μm. The rotation step is 0.4° over 180° degrees. We perform here what can be called a fast scan, in a total of about 2 h per sample. Since the objects are larger than the field of view of the detector, several sets of radiograms are taken and stitched together. The final projections are actually mosaics of 3 by 2 radiograms, meaning that one set of radiograms is acquired in about 20 min, which is relatively fast. In fact, the aim of this procedure is to have a good compromise between the acquisition quality, time, and number of samples.

Image reconstruction

Reconstruction is performed with the NRecon software[®] supplied with the Skyscan Micro-CT system. Ring artefact correction and rotation axis misalignment compensation is used. The resulting cross-sections are then stacked and imported in Avizo[®] to be processed.

Image processing

In order to process our microtomograms, we use an algorithm developed by Plougonven (2009) and integrated in the Avizo[®] software. This algorithm is organized in two steps, a pre-processing of the images (noise reduction thanks to a greyscale opening, followed by a Gaussian filtering) and a post-processing to decompose the porosity into individual pores, and calculate morphological parameters. Between these two steps, a threshold value needs to be chosen. We apply a single threshold value based on the Otsu's method (1979) for all our samples, the scanning and reconstruction parameters being identical (Beckers et al., 2012).

Post-process

Once the threshold value is chosen, the part of the algorithm calculating morphological parameters can be applied in Avizo[®]. It provides local 3-D quantification based on pore space decomposition – using skeletonization and a modified watershed method- (Plougonven, 2009): volume (Vol), surface, barycentre, inertia tensor, number of neighboring pores (N_c), surface area of the connections (Sf_c) and equivalent radius. Additionally, we compute the specific surface (SS) for each pore, and the pore deformation (Def), defined as the ratio between minimum and maximum components of the inertia tensor. Using this deformation, an elliptic cylinder was fitted to the pores in order to calculate a mean radius (R). Finally, we calculate a variable related to specific connectivity (SC):

$$SC = \frac{N_c \cdot A_c}{V_p} \quad (4)$$

Where N_c is the number of connections, A_c the mean surface area of the connections (L^2) and V_p the pore volume (L^3).

2.3 Measurements analysis

2.3.1 Retention and hydraulic functions

Continuous retention and hydraulic functions can be adjusted on our data points. Numerous models exist. Since we study the near saturation behaviour, this part of the curve will be of great importance. According to Durner (1994), the largest differences in retention and hydraulic predictions are not caused by the choice of the single porosity model, but by taking into account – or not – supplementary pore systems. In such a context, one model of each type has been adjusted: the unimodal from van Genuchten (1980) and the bimodal from Durner (1994). The associated hydraulic model is Mualem (1976) for both cases.

HESSD

10, 4799–4827, 2013

A method to enhance near saturation functions?

E. Beckers et al.

Title Page

Abstract

Introduction

Conclusions

References

Tables

Figures

◀

▶

◀

▶

Back

Close

Full Screen / Esc

Printer-friendly Version

Interactive Discussion



The van Genuchten formulation is:

$$\theta(h) = \theta_r + \frac{\theta_s - \theta_r}{[1 + |\alpha h|^n]^m} \quad (5)$$

With θ_r the residual water content, θ_s the saturated water content, n a pore size distribution parameter, α the inverse of the bubbling pressure (L^{-1}) and m a function of n ($m = 1 - 1/n$). The associated hydraulic conductivity is expressed as follow (Mualem, 1976):

$$K(h) = K_s S_e^l \left[1 - \left(1 - S_e^{1/m} \right)^m \right]^2 \quad (6)$$

With K_s the saturated hydraulic conductivity (LT^{-1}), l a pore connectivity parameter, and S_e the effective saturation:

$$S_e = \frac{\theta - \theta_r}{\theta_s - \theta_r} \quad (7)$$

With the Dual Porosity model (Durner, 1994) the effective saturation becomes:

$$S_e = w_1 [1 + (\alpha_1 h)^{n_1}]^{-m_1} + w_2 [1 + (\alpha_2 h)^{n_2}]^{-m_2} \quad (8)$$

With w the weighing factor, suffixes 1 and 2 referring to each part of the porosity. And the hydraulic function:

$$K(S_e) = K_s \frac{(w_1 S_{e1} + w_2 S_{e2})^l \left(w_1 \alpha_1 \left[1 - \left(1 - S_{e1}^{1/m_1} \right)^{m_1} \right] + w_2 \alpha_2 \left[1 - \left(1 - S_{e2}^{1/m_2} \right)^{m_2} \right] \right)^2}{(w_1 \alpha_1 + w_2 \alpha_2)^2} \quad (9)$$

HESSD

10, 4799–4827, 2013

A method to enhance near saturation functions?

E. Beckers et al.

Title Page

Abstract

Introduction

Conclusions

References

Tables

Figures

◀

▶

◀

▶

Back

Close

Full Screen / Esc

Printer-friendly Version

Interactive Discussion



2.3.2 Principal component analysis

Principal component analysis (PCA) has been widely described in the literature, for example in Benzécri and Benzécri (1980) cited by Palm (1994), or in Jackson (1991). PCA is a multivariate descriptive method. It aims at gathering descriptive parameters in a few components. The use of these components allows a 2-D representation of the data and highlights possible relationships between data and parameters. As Jackson (1980) said: “This method is used to simplify the simultaneous interpretation of a number of related variables”.

3 Results and discussion

3.1 Penetrometry

Figure 1 illustrates soil resistance to penetration for the CT and RT plots. We can observe two different soil horizons for both practices. In the CT profile, the second horizon appears at approximately 30 cm. The upper layer, from 0 to 30 cm, is quite homogeneous with a slight gradient along the depth. In the RT profile, the second horizon appears between 10 and 15 cm. The old plough pan is still observed at 30 cm depth. The sampling campaign is illustrated as well.

3.2 Retention functions

For the retention curves, the three horizons were analyzed: CT, RT1 (0–10 cm depth) and RT2 (12–25 cm depth). We used either the van Genuchten (1980) equation (VG) or the Dual Porosity (DP) model (Durner, 1994) to fit the data points. First, fitting is applied to Richards’ measurements alone (“R”). In a second step, fitting is applied to a combination of Richards’ (from pF 4.2 to pF 1) and μ CT data (from pF 1 to saturation) (called “ μ CT + R”).

HESSD

10, 4799–4827, 2013

**A method to
enhance near
saturation functions?**

E. Beckers et al.

Title Page

Abstract

Introduction

Conclusions

References

Tables

Figures

⏪

⏩

◀

▶

Back

Close

Full Screen / Esc

Printer-friendly Version

Interactive Discussion



With the R fitting (cf. Fig. 2, dotted lines), Relative Root Mean Square Errors (RRMSE) are better with the DP model for CT and RT2 but not for RT1 (cf. Table 1), differences between VG and DP performances being quite important for CT.

Comparing the horizons with DP, the only significant difference concerns the total effective porosity: it is greater for CT than for RT2. RT1 is in between, but differences are not significant. We can see that near saturation, curves present different shapes. But the curves for RT are not well fitted for this part, especially for RT1.

The combination of Richards and μ CT data is also fitted with the VG and DP models (cf. Fig. 2, solid lines). First, we can see that RRMSE (cf. Table 1) are widely better for the DP models than the VG ones. In fact, the VG model can fit either Richards' data or μ CT data, but fails in fitting a coupled data set.

Looking at the DP curves, volumes from pF 1 to saturation are not significantly different for the horizons. But we can see that for RT2, this volume is more important than with Richards measurements ($p < 0.05$) while for CT and RT1 these volumes match. Considering this match and the elements of the image analysis pre-process (see Sect. 2.2.4), obviously Richards' procedure does not allow a good saturation estimation for RT2. The reason could be linked to the pore distribution.

We can also observe that the DP fit on R and both VG fits have quite the same global shape around saturation, but not CT and RT1 μ CT + RDP curves. Indeed, comparing DP retention curves designed with μ CT + R and designed with R, we observe that for CT and RT1, concavity is inverted from pF 1.2 to saturation. With μ CT, the main part of the volume is closer to saturation than with R: for CT curve, the volume increase begins around pF 1 and slows down around pF 0 with R, while with μ CT the volume increase begins around pF 0.6 and stops around pF -0.06. As a result, μ CT data shows more pores with a bigger radius. These conclusions are the same for RT1 and RT2. For RT1, μ CT increase is even closer to saturation and consequently we have more and bigger pores than in CT. Furthermore for RT2, it confirms that fitting on R data leads to a bad approximation of porosity at saturation.

HESSD

10, 4799–4827, 2013

A method to enhance near saturation functions?

E. Beckers et al.

Title Page

Abstract

Introduction

Conclusions

References

Tables

Figures

⏪

⏩

◀

▶

Back

Close

Full Screen / Esc

Printer-friendly Version

Interactive Discussion



3.3 Hydraulic conductivity

3.3.1 Hydraulic macroporosity efficiency

If we compare macroporosity estimated from Ksat measurements (θ_M) vs. macroporosity estimated from Richards' and μ CT measurements, we can use the ratio of these values as an indicator of macroporosity efficiency (ER) – in terms of conductivity ability – and pore network morphology. For both cases, we obtain the following results: CT > RT2 > RT1 (cf. Table 2), with the latter being the most distant from Poiseuille's law with respect to structure morphology, i.e. reflecting poor dynamic performances. In fact, RT1 presents the higher near saturation pore volume while its saturated hydraulic conductivity is the lowest.

3.3.2 Hydraulic functions

Using Ksat measured with the permeameter and results from fitted parameters with retention data, $K(h)$ curves with the 4 different adjustments are represented in Fig. 3 for each horizon. Tensio-infiltrimeter (TI) measurements are indicated as well, and the match between these points and fitting curves are calculated. For RT1 and RT2, the same TI measurements are used. In fact, because of the lower depth of RT1 in regard with CT, measurements cannot be attributed exclusively to RT1.

Comparing fitted models, we can see that for CT the unsaturated flow prediction is particularly enhanced when taking into account the presence of a secondary pore system (cf. Table 3). For RT2, the greater improvement is due to the μ CT complementary data. But in both cases, it is the combination of μ CT data and the DP model that gives the best prediction of the unsaturated flow. It seems to validate the adjustment of elliptic cylinders to obtain pore size distribution.

Concerning RT1, results are quite the same for “ μ CT + R” data with VG and DP models, the better prediction being for R DP. The poor match for RT1 is probably caused by two factors. First, the TI measurements are probably more representative of RT2,

HESSD

10, 4799–4827, 2013

**A method to
enhance near
saturation functions?**

E. Beckers et al.

Title Page

Abstract

Introduction

Conclusions

References

Tables

Figures

◀

▶

◀

▶

Back

Close

Full Screen / Esc

Printer-friendly Version

Interactive Discussion



and this is confirmed by the excellent match for this horizon. Secondly, the DP retention curve on combined data does not fit very well between pF 0 and saturation. RT1 measurements present a great variability especially in this pressure range; therefore the mean curve might not be representative of the mean behaviour. In fact, Durner et al. (1999) mention the possible difficulty to average dual porosity curves in some cases.

We can see that both fittings on R and $\mu\text{CT} + R$ with the DP model allow a better adjustment for retention curves. Our results show that for R retention curves DP improves the fitting, but not significantly. In fact, without complementary information, it is difficult to choose a model. It is generally accepted that unimodal models – like VG – are adequate and, because of their easier implementation, are therefore often preferred (Durner et al., 1999). But in our case, the DP model proves to better predict the unsaturated conductivity. This is supported by results of Durner et al. (1999) on silty soils. They show that the more parameters are involved, the better the fitting on hydraulic functions, i.e. multimodal models.

Besides, μCT data allow refining retention and hydraulic curves near saturation where Richards' data alone can lead to numerous sets of fitted parameters. However, other methods allow this as well (for example, Hyprop apparatus, UMS[®]). But microtomographic images processed with an appropriate algorithm may be more powerful. Matching micro and macroscopic measurements allows us to validate μCT information, which is not so obvious (Baveye et. al, 2010). And the algorithm we use (Plougonven, 2009) proves to be effective separating pores individually since both retention and conductivity functions present an enhancement. The next step is therefore to make use of potential structural information on individual pores.

3.4 X-ray microtomography: principal component analysis

Principal component analysis (PCA) is performed on our samples, taking into account 7 parameters (cf. Sect. 2.2.4.): Vol, N_c , Sf_c , SS, R, Def and SC. The first 3 components explain about 90 % of the variability between samples, F1 (first component)

A method to enhance near saturation functions?

E. Beckers et al.

Title Page

Abstract

Introduction

Conclusions

References

Tables

Figures

⏪

⏩

◀

▶

Back

Close

Full Screen / Esc

Printer-friendly Version

Interactive Discussion



explaining alone 54 % of the variability. All seven parameters are well correlated at least for one component. We represent in Fig. 4 and Fig. 5 the results for pores with a radius $> 1500 \mu\text{m}$ ($h > -1 \text{ cm}$), because of their bigger influence on hydrodynamic behaviour. CT and RT2 are in opposition with RT1 along F1. RT1 and RT2 differ because of a lower surface of connections and a bigger specific surface for RT2, while RT1 and CT are disconnected because of larger volume and radius, and a lower specific surface for RT1. While mean object positions do not underline great differences, we can still observe along F1 the ranking $\text{CT} < \text{RT2} < \text{RT1}$, which is the inverse than for macroporosity conductivity efficiency. We can see that for tilled soils it is not only the macropore volume that influences conductivity but also topological parameters such as specific surface and specific connectivity – which are highly correlated with F1. This agrees with results from Vogel and Roth (1998) who demonstrate that realistic pore network representation has to take into account its connectivity and tortuosity. We confirm here that specific surface and specific connectivity would therefore represent interesting structural parameters to refine hydraulic functions characterization.

In addition to the conclusions about the mean topological parameters, the horizon intra-variability provides supplementary clues. In fact, the dispersion coefficient is very low for CT. It is important for RT2, but because of one sample alone, while RT1 is characterized by a dispersed spatial position of the samples. This behaviour seems to be symptomatic for this horizon. If we analyze macroscopic measurements with this point of view, we can see that the horizons present the same characteristics as above about variability. CT has a low variation range and its mean and median are often superimposed. RT2 has as well a low variation range, but its mean is displaced because of a few outliers. And finally RT1 presents the higher variation range and big differences between mean and median.

We could conclude that the poor dynamic performances – reflected by ratio between macroporosity and saturated hydraulic conductivity – for RT1 can be linked with this great heterogeneity (and therefore agrees with the divergence found in the literature, e.g. Strudley et al., 2008), while for RT2 it is more related to a generally low permeable

HESSD

10, 4799–4827, 2013

A method to enhance near saturation functions?

E. Beckers et al.

Title Page

Abstract

Introduction

Conclusions

References

Tables

Figures

◀

▶

◀

▶

Back

Close

Full Screen / Esc

Printer-friendly Version

Interactive Discussion



medium. However, outliers seem to be a rule in RT2 populations, one of the main reasons probably being a greater microfaunistic activity – which is in concordance with results of Cousin et al. (2004). In fact, microfauna produces large pores which can be observed with μ CT and permeability measurements – but scarcely are – because of the size of the samples. While Richards’ measurements are not able to detect them because of the difficulty of entirely saturating macroporosity.

4 Conclusions

This work is an initial validation of microtomographic results obtained with a relative quick scan method. The good match for both retention and conductivity functions with macroscopic measurements validates the μ CT information, not only globally but also locally, since the macroscopic measurements match the pore volume distribution produced by radius determination and classification through the adjustment of an elliptic cylinder. In this case, microtomography proves to be a very promising tool. Richards’ measurements supply a double porosity fitted retention curve, but is not so distinct from the classical van Genuchten model, while combination of μ CT data and DP model can confirm the presence of this secondary pore system and expands our knowledge of the near saturation pore distribution. Besides, where macroscopic measurements give a first insight on the comparison between management practices, μ CT data allows pore visualization and characterization. Notably, μ CT highlights the presence of bigger pores since the retention function presents an inverted concavity from Richards’ curve. Analysis of structural parameters for these pores appears to be significant and offers an additional step in objects differentiation. PCA shows that 7 structural parameters can explain nearly 90 % of the variability between horizons, and that they are important to differentiate them. The most determining parameters in our context are specific surface, specific connectivity, volume and radius. They are able to explain and help determine transport phenomena: specific surface is useful in solute transfer modelling,

HESSD

10, 4799–4827, 2013

A method to enhance near saturation functions?

E. Beckers et al.

Title Page

Abstract

Introduction

Conclusions

References

Tables

Figures

◀

▶

◀

▶

Back

Close

Full Screen / Esc

Printer-friendly Version

Interactive Discussion



and those related to connectivity characterization are potentially useful to refine conductivity function knowledge and could thus help to predict conductivity.

Note that with X-ray tomography, the acquired images can constitute a growing database, and that new algorithms can be applied and tested repeatedly.

5 References

- Attix, F. H. R. and Roesch, W. C.: Radiation Dosimetry, Academic Press, New York, 1968.
- Baveye, P. C., Laba, M., Otten, W., Bouckaert, L., Dello Sterpaio, P., Goswami, R. R., Grinev, D., Houston, A., Hu, Y., Liu, J., Mooney, S., Pajor, R., Sleutel, S., Tarquis, A., Wang, W., Wei, Q., and Sezgin, M.: Observer-dependent variability of the thresholding step in the quantitative analysis of soil images and X-ray microtomography data, *Geoderma*, 157, 51–63, 2010.
- Bayer, A., Vogel, H.-J., and Roth, K.: Direct measurement of the soil water retention curve using X-ray absorption, *Hydrol. Earth Syst. Sci.*, 8, 2–7, doi:10.5194/hess-8-2-2004, 2004.
- Beckers, E., Roisin, C., Plougonven, E., Deraedt, D., Léonard, A., and Degré, A.: Micro and macroscopic investigation to quantify tillage impact on soil hydrodynamic behaviour, *Geophys. Res. Abstr.*, EGU2012-2033, EGU General Assembly 2012, Vienna, Austria, 2012.
- Bhattacharyya, R., Prakash, V., Kundu, S., and Gupta, H. S.: Effect of tillage and crop rotations on pore size distribution and soil hydraulic conductivity in sandy clay loam soil of the Indian Himalayas, *Soil Till. Res.*, 86, 129–140, 2006.
- Cousin, I., Vogel, H.-J., and Nicoullaud, B.: Influence de la structure du sol à différentes échelles sur les transferts d'eau : conséquences d'une réduction du travail du sol, *Étude Gestion Sols*, 11, 69–81, 2004.
- Dal Ferro, N., Delmas, P., Duwig, C., Simonetti, G., and Morari, F.: Coupling X-ray microtomography and mercury intrusion porosimetry to quantify aggregate structures of a cambisol under different fertilisation treatments, *Soil Till. Res.*, 119, 13–21, 2012.
- Durner, W.: Hydraulic conductivity estimation for soils with heterogeneous pore structure, *Water Resour. Res.*, 30, 211–233, 1994.
- Durner, W., Priesack, E., Vogel, H. J., and Zurmühl, T.: Determination of parameters for flexible hydraulic functions by inverse modeling, in: *Proc. Int. Workshop, Characterization and Measurement of the Hydraulic Properties of Unsaturated Porous Media*, edited by: van

HESSD

10, 4799–4827, 2013

A method to enhance near saturation functions?

E. Beckers et al.

[Title Page](#)

[Abstract](#)

[Introduction](#)

[Conclusions](#)

[References](#)

[Tables](#)

[Figures](#)

[⏪](#)

[⏩](#)

[◀](#)

[▶](#)

[Back](#)

[Close](#)

[Full Screen / Esc](#)

[Printer-friendly Version](#)

[Interactive Discussion](#)



HESSD

10, 4799–4827, 2013

A method to enhance near saturation functions?

E. Beckers et al.

[Title Page](#)[Abstract](#)[Introduction](#)[Conclusions](#)[References](#)[Tables](#)[Figures](#)[◀](#)[▶](#)[◀](#)[▶](#)[Back](#)[Close](#)[Full Screen / Esc](#)[Printer-friendly Version](#)[Interactive Discussion](#)

Genuchten, M. T., Leij, F. J., and Wu., L., University of California, Riverside, CA, 817–830, 1999.

Gerke, H. H.: Macroscopic representation on of the interface between flow domains in structured soil, *Vadose Zone J.*, 11, 3, doi:10.2136/vzj2011.0125, 2012.

5 Green, T. R., Ahujaa, L. R., and Benjamin, J. G.: Advances and challenges in predicting agricultural management effects on soil hydraulic properties, *Geoderma*, 116, 3–27, 2003.

Imhoff, S., Ghiberto, P. J., Grioni, A., and Gay, J. P.: Porosity characterization of Argiudolls under different management systems in the Argentine Flat Pampa, *Geoderma*, 158, 268–274, 2010.

10 Jackson, J. E.: Principal components and factor analysis: part I-principal components, *J. Qual. Technol.*, 12, 201–213, 1980.

Jackson, J. E.: *A User's Guide to Principal Components*, Wiley, New York, 1991.

Kim, H., Anderson, S. H., Motavalli, P. P., and Gantzer, C. J.: Compaction effects on soil macropore geometry and related parameters for an arable field, *Geoderma*, 160, 244–251, 2010.

15 Kumar, S., Anderson, S. H., and Udawatta, R. P.: Agroforestry and grass buffer influences on macropores measured by computed tomography under grazed pasture systems, *Soil Sci. Soc. Am. J.*, 74, 203–212, 2010.

Mualem, Y.: A new model for predicting the hydraulic conductivity of unsaturated porous media, *Water Resour. Res.*, 12, 513–522, 1976.

20 Olsen, P. A. and Borresen, T.: Measuring differences in soil properties in soils with different cultivation practices using computer tomography, *Soil Till. Res.*, 44, 1–12, 1997.

Otsu, N.: A threshold selection method from gray-level histograms, *IEEE Sys. Man Cybern.*, 9, 62–66, 1979.

25 Palm, R.: *Les méthodes d'analyse factorielle : principes et applications*, *Biom. Praxim.*, 34, 35–80, 1994.

Plougonven, E.: *Lien entre la microstructure des matériaux poreux et leur perméabilité : Mise en évidence des paramètres géométriques et topologiques influant sur les propriétés de transport par analyses d'images microtomographiques*, Ph.D. Thesis, Université Bordeaux 1, Bordeaux, France, 116 pp., 2009.

30 Quinton, W. L., Elliot, T., Price, J. S., Rezanezhad, F., and Heck, R.: Measuring physical and hydraulic properties of peat from X-ray tomography, *Geoderma*, 153, 269–277, 2009.

A method to enhance near saturation functions?

E. Beckers et al.

Title Page

Abstract

Introduction

Conclusions

References

Tables

Figures

⏪

⏩

◀

▶

Back

Close

Full Screen / Esc

Printer-friendly Version

Interactive Discussion



Rachman, A., Anderson, S. H., and Gantzer, C. J.: Computed tomographic measurement of soil macroporosity parameters as affected by stiff-stemmed grass hedges, *Soil Sci. Soc. Am. J.*, 69, 1609–1616, 2005.

Richards, L. A.: Porous plate apparatus for measuring moisture retention and transmission by soils, *Soil Sci.*, 66, 105–110, 1948.

Roisin, C.: A multifractal approach for assessing the structural state of tilled soils, *Soil Sci. Soc. Am. J.*, 71, 15–25, 2007.

Solone, R., Bittelli, M., Tomei, F., and Morari, F.: Errors in water retention curves determined with pressure plates: effects on the soil water balance, *J. Hydrol.*, 470–471, 65–74, 2012.

Strudley, M. W., Green, T. R., and Ascough, J. C.: Tillage effects on soil hydraulic properties in space and time: state of the science, *Soil Till. Res.*, 99, 4–48, 2008.

Taina, I. A., Heck, R. J., and Elliot, T. R.: Application of X-ray computed tomography to soil science: a literature review, *Can. J. Soil Sci.*, 88, 1–20, 2008.

van Genuchten, M. T.: A closed-form equation for predicting the hydraulic conductivity of unsaturated soils, *Soil Sci. Soc. Am. J.*, 44, 892–898, 1980.

Vogel, H. J. and Roth, K.: A new approach for determining effective soil hydraulic functions, *Eur. J. Soil Sci.*, 49, 547–556, 1998.

Wiermann, C., Werner, D., Horn, R., Rostek, J., and Werner, B.: Stress/strain processes in a structured unsaturated silty loam Luvisol under different tillage treatments in Germany, *Soil Till. Res.*, 53, 117–128, 2000.

HESSD

10, 4799–4827, 2013

A method to enhance near saturation functions?

E. Beckers et al.

Table 1. RRMSE for fitting Richards' data set (R) and combined data set (μ CT + R) with van Genuchten (VG) or Dual Porosity (DP) model.

Horizon	"R" VG	"R" DP	" μ CT + R" VG	" μ CT + R" DP
CT	0.035	0.016	0.036	0.013
RT1	0.039	0.044	0.048	0.012
RT2	0.026	0.020	0.045	0.004

[Title Page](#)[Abstract](#)[Introduction](#)[Conclusions](#)[References](#)[Tables](#)[Figures](#)[|◀](#)[▶|](#)[◀](#)[▶](#)[Back](#)[Close](#)[Full Screen / Esc](#)[Printer-friendly Version](#)[Interactive Discussion](#)

A method to enhance near saturation functions?

E. Beckers et al.

Table 2. K_s = saturated hydraulic conductivity; N_M = number of hydraulically effective pores; θ_M = hydraulically effective macroporosity; ER = efficiency ratios for μ CT (T) and Richards' (R) measurements (m)

Horizon	K_s (ms^{-1})	N_M	θ_M	ER T(m)	ER R(m)
CT	1.6×10^{-4}	$8.1 \times 10^{+4}$	7.0×10^{-1}	1.2×10^{-1}	1.1×10^{-1}
RT1	2.5×10^{-5}	$1.3 \times 10^{+4}$	1.1×10^{-1}	2.3×10^{-2}	2.0×10^{-2}
RT2	4.0×10^{-5}	$2.0 \times 10^{+4}$	1.8×10^{-1}	3.8×10^{-2}	7.2×10^{-2}

[Title Page](#)
[Abstract](#)
[Introduction](#)
[Conclusions](#)
[References](#)
[Tables](#)
[Figures](#)
[Back](#)
[Close](#)
[Full Screen / Esc](#)
[Printer-friendly Version](#)
[Interactive Discussion](#)


HESSD

10, 4799–4827, 2013

A method to enhance near saturation functions?

E. Beckers et al.

Table 3. RRMSE for fitting Richards' data set (R) and combined data set (μ CT + R) with van Genuchten (VG) or Dual Porosity (DP) model

Horizon	"R" VG	"R" DP	" μ CT + R" VG	" μ CT + R" DP
CT	5.2	0.4	4.2	0.2
RT1	1.9	0.3	0.9	1.0
RT2	25.7	17.2	3.2	0.8

[Title Page](#)[Abstract](#)[Introduction](#)[Conclusions](#)[References](#)[Tables](#)[Figures](#)[|◀](#)[▶|](#)[◀](#)[▶](#)[Back](#)[Close](#)[Full Screen / Esc](#)[Printer-friendly Version](#)[Interactive Discussion](#)

HESSD

10, 4799–4827, 2013

A method to enhance near saturation functions?

E. Beckers et al.

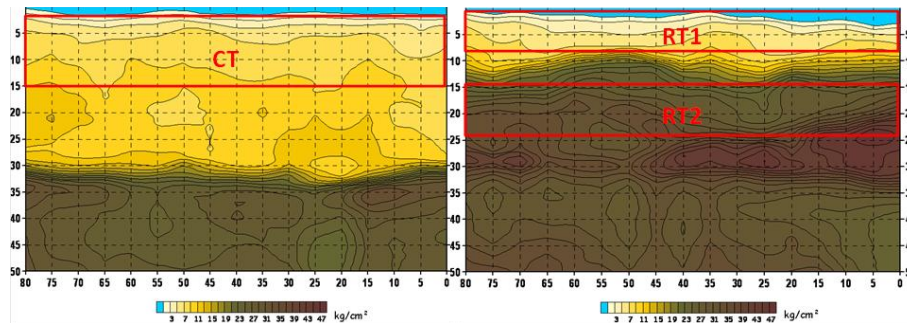


Fig. 1. 3-D soil strength profiles. Left: CT profile; right: RT profile.

Title Page

Abstract

Introduction

Conclusions

References

Tables

Figures

◀

▶

◀

▶

Back

Close

Full Screen / Esc

Printer-friendly Version

Interactive Discussion



A method to enhance near saturation functions?

E. Beckers et al.

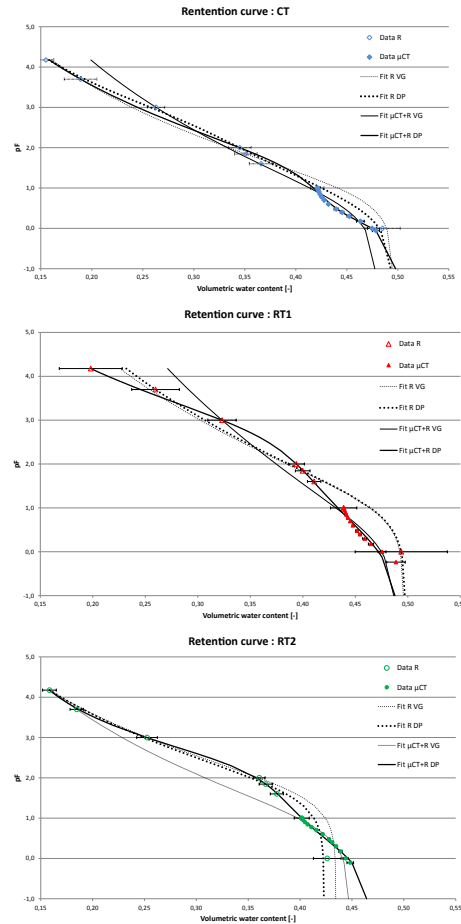


Fig. 2. Retention curves. Dotted line: Richards' measurements (R); solid line: combined μ CT and Richards' measurements (μ CT + R); fine line: van Genuchten adjustment (VG); thick line: Dual Porosity adjustment (DP).

[Title Page](#)
[Abstract](#)
[Introduction](#)
[Conclusions](#)
[References](#)
[Tables](#)
[Figures](#)
[Back](#)
[Close](#)
[Full Screen / Esc](#)
[Printer-friendly Version](#)
[Interactive Discussion](#)


A method to enhance near saturation functions?

E. Beckers et al.

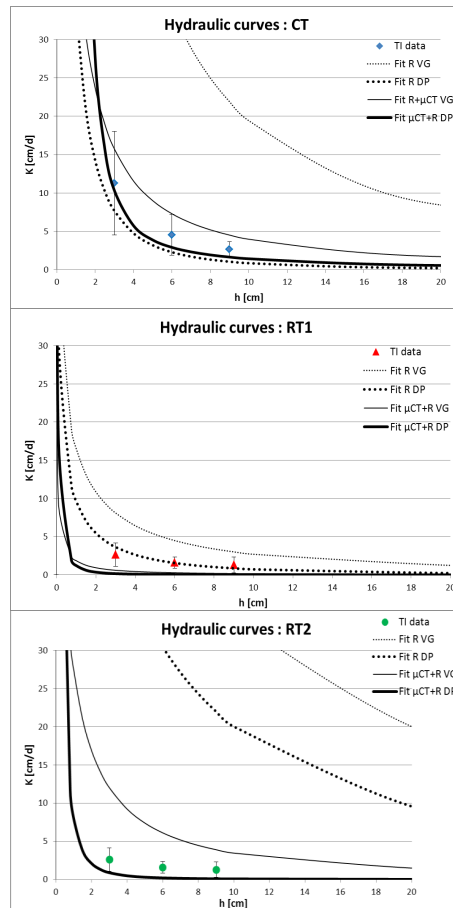


Fig. 3. Hydraulic curves. Dotted line: Richards' measurements (R); solid line: combined μ CT and Richards' measurements (μ CT + R).

Title Page

Abstract

Introduction

Conclusions

References

Tables

Figures

⏪

⏩

⏴

⏵

Back

Close

Full Screen / Esc

Printer-friendly Version

Interactive Discussion



A method to enhance near saturation functions?

E. Beckers et al.

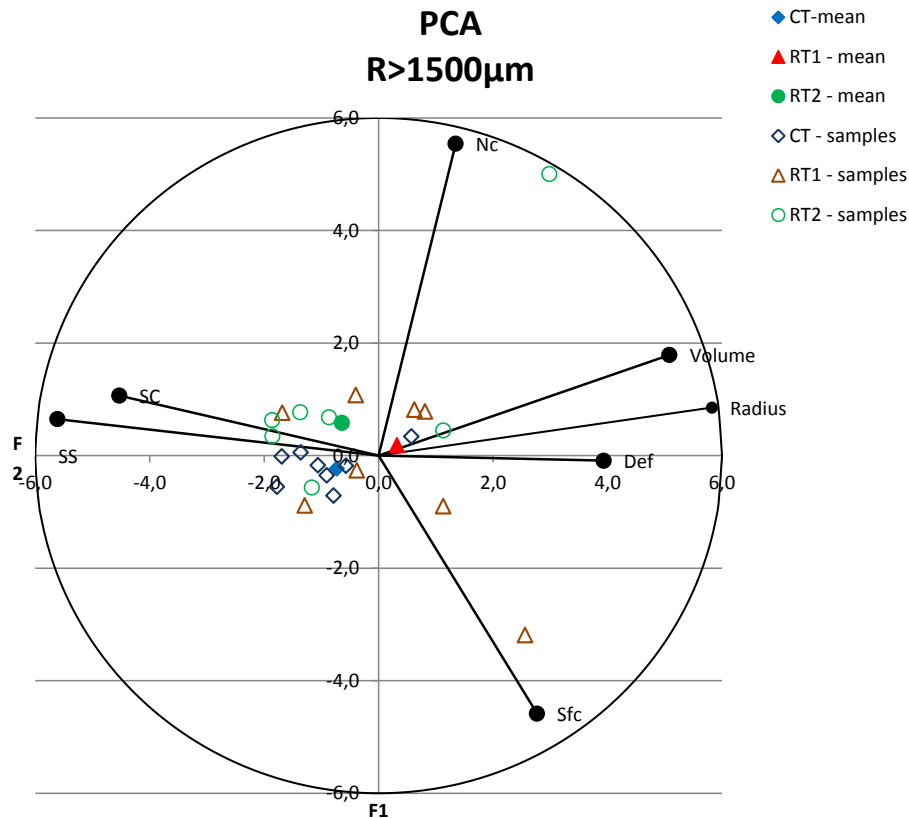


Fig. 4. PCA scores for pores with $r > 1500 \mu\text{m}$ – F1 (54 %); F2 (23 %).

Title Page

Abstract Introduction

Conclusions References

Tables Figures

⏪ ⏩

⏴ ⏵

Back Close

Full Screen / Esc

Printer-friendly Version

Interactive Discussion



A method to enhance near saturation functions?

E. Beckers et al.

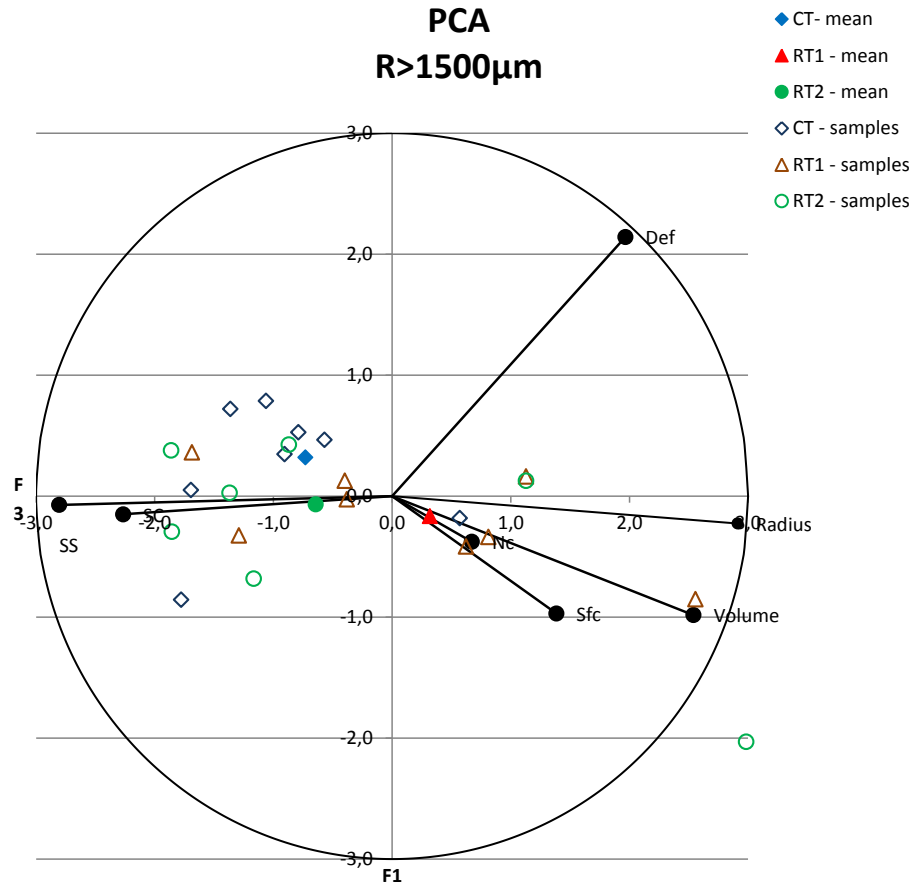


Fig. 5. PCA scores for pores with $r > 1500 \mu\text{m}$ – F1 (54%); F3 (11%).

Title Page

Abstract Introduction

Conclusions References

Tables Figures

⏪ ⏩

⏴ ⏵

Back Close

Full Screen / Esc

Printer-friendly Version

Interactive Discussion

